

**A.F. Nazarenko, T.M. Sliozberg, A.A. Nazarenko**

**VORTEX CONFIGURATION WITHIN SOUNDGENERATIVE ELEMENT OF HYDRODYNAMIC EMITTING SYSTEM**

Odessa State Polytechnic University  
1, Shevchenko av., Odessa, 65044, Ukraine  
Tel.: (0482) 288-480

Odessa National I.I. Mechnikov University  
42, Pastera str., Odessa, 65026, Ukraine  
Tel.: (0482) 633-633

*The elaborated model of sound generation at aerodynamical emitter with cavitation sound generative element allows to determine the generated acoustical vibrations' main spectral frequency by the methods of solving a transcendent dispersion equation. This solution is in close relationship with the mass of a toroidal vortex, shaped by the liquid influent into sound generative element, i.e. the solution depends upon this vortex' configuration. To find experimentally, which of possible configurations number is realized within hydrodynamical emitter is not a result of high probability. The study provided seeks the basic configurations' frequencies calculations the outcomes being compared with the found experimentally frequencies. The investigations revealed that among the variances sought there exists an unique one providing results accordingly to the experiment, the rest variances being in its contradiction. The conclusion issuing from these outcomes considers the vortex' configuration realized at an hydrodynamic emitter.*

The hydrodynamic emitting systems application in capacity of sources of acoustical oscillations for technological purposes is of high preference when compared to the magnetostrictional and piezoelectric emitters because of many reasons. In this connection, the modelling of complex hydrodynamic and acoustical processes, having place when these emitters generate the vibrations, represents not only scientific but also applied spheres of interest.

The sound generative element at the sought emitters consists in cavitation area, which localization is provided by submerged liquid jet, effluent from circular slot nozzle and affluent onto a flat barrier [1]. A part of flow discharge arrives inside of the shaped cylindrical hollow jet, the discharge's vortex-like motion onto the toroidal surface exciting the cavitation effect. The liquid injection into this area continues until the inner overpressure produce an abrupt release of cavity's content into environment. These repeating releases' periodicity prescribes the main tone frequency within complex spectrum of vibrations, propagating at liquid.

These processes mathematical description can be reduced to the cylindrical jet motion differential equation solution, the motion being supposed a harmonic oscillation, and that solution-issuing dispersion equation, establishing relations between the vibrations' frequency and emitting system geometrical both hydrodynamic parameters. This equation will be [1]:

$$h = \sqrt{2\Gamma} \sin \frac{h}{2}. \quad (1)$$

The model simplest variance (disregard of submerged jet expanding, due to Bernoulli effect) being nevertheless, the boundary condition reflecting the actual processes essential features, the formula (1) parameters will represent the following content [1]:

$$h = \frac{2\mathbf{p} f l}{v_0}; \quad \Gamma = 2\mathbf{x} \left[ \frac{\mathbf{c}}{\mathbf{m}} \cdot \frac{P_0}{r v_0^2} + \frac{\mathbf{p} r_0 l^2 \mathbf{r}}{m_a} \right]; \quad (2)$$

where  $f$  – vibrations frequency;  $v_0$  – speed of nozzle-effluent liquid;  $l$  – distance between the nozzle and barrier flanks;  $\xi$  – part of affluent onto barrier flow discharge arriving inside of the cavity;  $\chi$  – proportional coefficient for supposed speed of cavity internal pressure change when liquid injecting;  $\mu$  – part of cylindrical volume between the nozzle and barrier flanks, occupied with cavitation area;  $P_0$  – surrounding liquid pressure;  $\rho$  – liquid density;  $r_0$  – circular slot nozzle average radius;  $m_a$  – vortex' mass.

As to parameter  $\eta$ , connected with vibrations frequency, the equation (1) is transcendental one. Its solution is very crucial with respect to  $\Gamma$  parameter, depending (as formula (2) indicates) onto vortex' mass  $m_a$ . So, there arises the problem of this vortex configuration. The reflected jet moves by inertia towards the nozzle flank, being warped with the affluent jet attraction due to the Bernoulli effect. When distances  $l$  are short comparatively with  $r_0$ , the assumption that the vortex' axial section radius  $R$  is prescribed by the distance between nozzle flank and the barrier (fig. 1.a; 2.a; 3,a) looks very logical one;

$$R \cong \frac{l}{2}. \quad (3)$$

When speaking about the  $l$  distances, exceeding the nozzle radius, we should make several different suppositions. The jet inertia can be sufficient for the case when jet arrives to the nozzle flank. Then the axial section radius will be as before, determined with formula (3), but the torus' inner region will undergo a partitive deformation (fig.1,b). Probably, the barrier affluent jet attraction influencing the reflected jet will result in reflected jet distortion up to its afflux onto nozzle flank. In that case, the vortex deformation is not actual and vortex' radius is determined by the circular slot nozzle radius:

$$R \cong \frac{r_0}{2}. \quad (4)$$

In this connection there exists probability of torus' axial sections centers several positions, id. e. its medial line radius different values. Two cases of this kind are shown at fig. 2,b and 3,b.

To found experimentally, which of these variances has place, is not possible. Therefore all these cases were sought and the calculations results being compared with corresponding experimental data, we came to conclusion of paramount occurrence for the case, proving the results, found in best accordance with the experiment.

The first case of "distorted vortex", shown at fig. 1, represents the torus' axial section radius prescribed by the formula (3) and its medial line radius

$$R_{c\delta} \cong \frac{r_0}{2}. \quad (5)$$

this vortex' mass and correspondingly,  $\tilde{A}$  parameter:

$$m_a \cong \frac{r p^2 r_0 l^2}{4}, \quad \tilde{A} = 2x \left[ \frac{c}{m} \cdot \frac{P_0}{r v_0} + \frac{4}{p} \right]. \quad (6)$$

The second case of "undistorted vortex", shown at fig. 2, represents the axial section radius:

$$R = \begin{cases} \frac{l}{2}, & l \leq r_0 \\ \frac{r_0}{2}, & l \geq r_0 \end{cases}, \quad (7)$$

and the torus' medial line radius is also calculated by formula (5). Here the vortex' mass and  $\Gamma$  parameter:

$$m_a = \begin{cases} \frac{r p^2 r_0 l^2}{4}, & l \leq r_0 \\ \frac{r p^2 r_0^3}{4}, & l \geq r_0 \end{cases}, \quad \Gamma = \begin{cases} 2x \left[ \frac{c}{m} \cdot \frac{P_0}{r v_0^2} \cdot \frac{l}{r_0} + \frac{4}{p} \right], & l \leq r_0 \\ 2x \left[ \frac{c}{m} \cdot \frac{P_0}{r v_0^2} \cdot \frac{l}{r_0} + \frac{4}{p} \cdot \frac{l^2}{r_0^2} \right], & l \geq r_0 \end{cases} \quad (8)$$

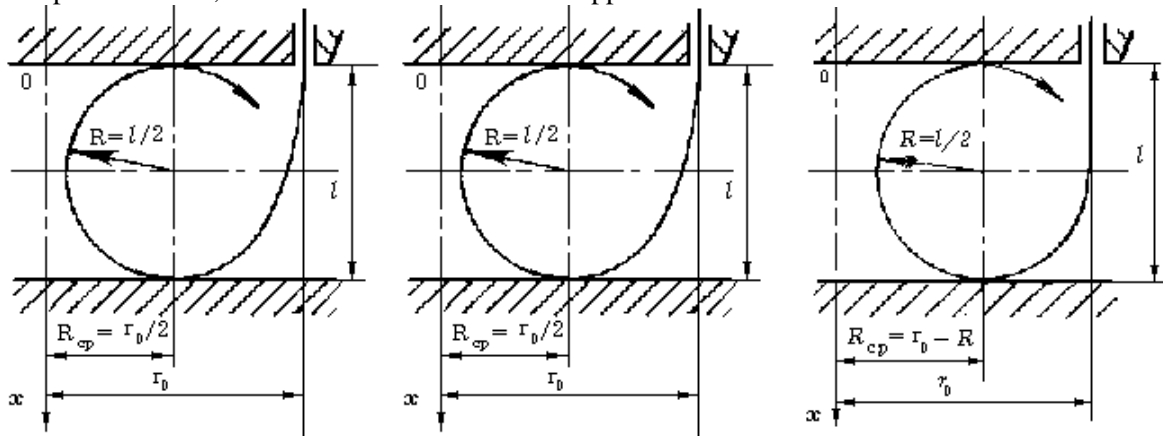
And, finally, the third case, this one also of "undistorted vortex" (fig. 3), when the axial section radius, as before, will be determined with the formula (7), and the medial line radius:

$$R_{\bar{n}\delta} \cong r_0 - R = \begin{cases} r_0 - \frac{l}{2}, & l \leq r_0 \\ \frac{r_0}{2}, & l \geq r_0 \end{cases}. \quad (9)$$

In that event the vortex' mass and  $\Gamma$  parameter are:

$$m_a'' = \begin{cases} \frac{rp^2 r_0 l^2}{4} \left(2 - \frac{l}{r_0}\right) & l \leq r_0 \\ \frac{rp^2 r_0^3}{4} & l \geq r_0 \end{cases}, \quad \Gamma'' = \begin{cases} 2x \left[ \frac{c}{m} \cdot \frac{P_0}{rv_0^2} \cdot \frac{l}{r_0} + \frac{4}{p} \cdot \frac{1}{2 - \frac{l}{r_0}} \right], & l \leq r_0 \\ 2x \left[ \frac{c}{m} \cdot \frac{P_0}{rv_0^2} \cdot \frac{l}{r_0} + \frac{4}{p} \cdot \frac{l^2}{r_0^2} \right], & l \geq r_0 \end{cases} \quad (10)$$

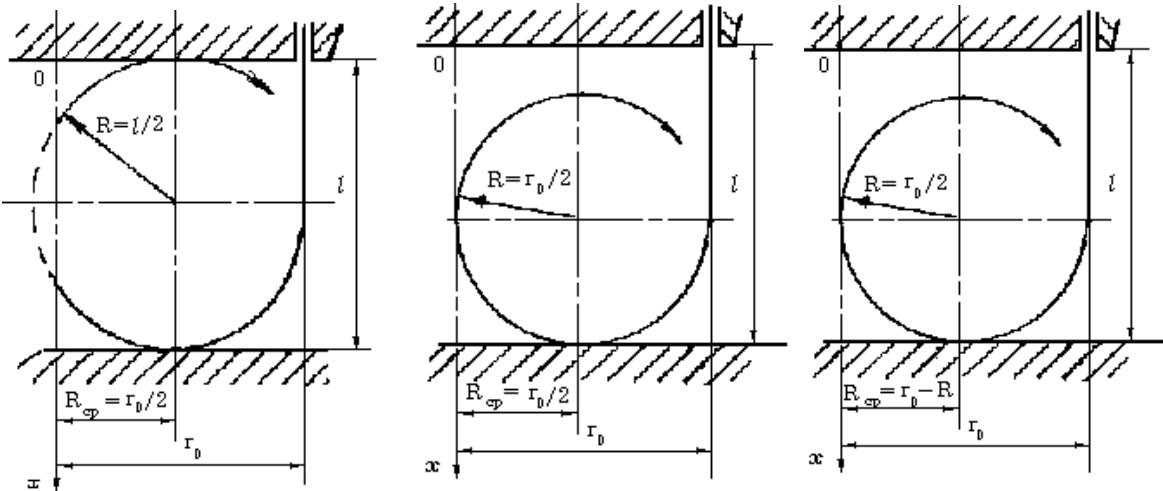
Whatever of these cases sought, the experimental dependency  $f(v_0)$  worked out by the methods described at work [1], got the averaged values for  $\xi$  and  $\chi$  parameters, serving to calculate the vibrations frequencies, generated under different  $l$  values (fig.4), the curve 1 – with the usage of (6) formulae; the curve 2 – when formulae (8) applied; and the curve 3 – by employing (10) formulae. The essentially best fitting between the experimental data curve 4 and the calculation results curve 1 when compared to the 2, 3 calculation results curves is apparent.



à)  $l < r_0$

à)  $l < r_0$

à)  $l < r_0$



b)  $l > r_0$

b)  $l > r_0$

b)  $l > r_0$

**Fig.1**

**Fig. 2**

**Fig.3**

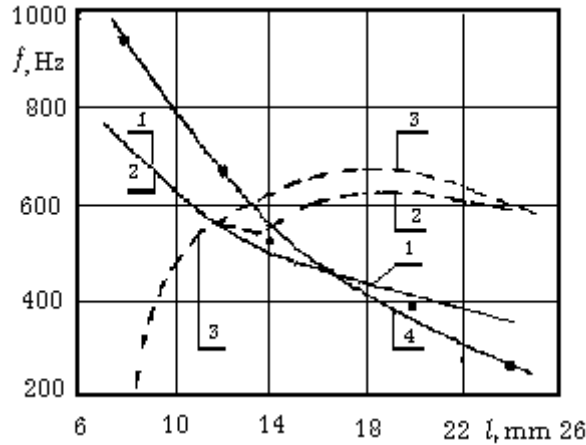


Fig. 4.

This evidence acknowledge the primary presidential realization of the “distorted vortex” model (fig.1). The indirect evidence confirming that conclusion consists in the fact that during experimental series, the most intensified sound generation is observed when the distance between the nozzle flank and the reflector does not exceed the nozzle radius. Just this correlation of  $l$  and  $r_0$  produce the dependency  $f(v_0)$ , serving as basis for  $\xi$  and  $\chi$  coefficients finding. The  $l$  distance increasing, the generated signal rate decreases. Probably, this effect reasons lay in the vortex “distortion” resulting from its separate parts’ mutual overlapping.

#### REFERENCE

1. Nazarenko A.A. Circular submerged fluid jet affluent onto a flat barrier autovibration.// RAO VI session. Acoustics on the XXI century threshold. Collected volume. M. 1997. P. 419-422 (in Russian)